

Nonlinear Viscoelastic Modeling for Foams

Veronika Effinger¹, Paul DuBois², Markus Feucht³,
André Haufe¹, Manfred Bischoff⁴

¹DYNAMore GmbH, Stuttgart, Germany

²Consultant, Offenbach, Germany

³Daimler AG, Sindelfingen, Germany

⁴Institute of Structural Mechanics, University of Stuttgart, Germany

Abstract

Lightweight design is one of the major principles in automotive engineering and has made polymer materials to inherent parts of modern cars. In addition to their lightweight potential thermoplastics, elastomers, fabric and composites also incur important functions in passive safety. In the age of virtual prototyping, assuring these functions requires the accurate modeling of the mechanical behavior of each component.

Due to their molecular structure, polymer materials often show viscoelastic characteristics such as creep, relaxation and recovery. However, considering the general state of the art in crash simulation, the viscoelastic characteristics are mainly neglected or replaced by viscoplastic or hyperelastic and strain rate dependent material models. This is either due to the available material models that are often restricted to linear viscoelasticity and thus cannot model the experimental data or due to the time consuming parameter identification.

*In this study, a nonlinear viscoelastic material model for foams is developed and implemented as a user material subroutine in LS-DYNA[®]. The material response consists of an equilibrium and a non-equilibrium part. The first one is modeled with a hyperelastic formulation based on the work of Chang [8] and formerly implemented as *MAT_FU_CHANG_FOAM in LS-DYNA (*MAT_083). The second one includes the nonlinear viscoelastic behavior following the multiple integral theory by Green and Rivlin [9].*

The polyurethane foam Confor[®] CF-45 used as part of the legform impactor in pedestrian safety was chosen for its highly nonlinear viscoelastic properties to test the presented approach. The investigation shows the ability of the method to reliably simulate some important nonlinear viscoelastic phenomena such as saturation.

Introduction

As its name implies, viscoelasticity is a combination of viscosity and elasticity. A viscoelastic solid shows instantaneous elasticity, stress relaxation under constant strain and creep under constant stress as illustrated in Figure 1.

In order to recognize viscoelastic material behavior no special experimental setup is necessary. If a viscoelastic material is subject to tensile tests at different strain rate and if the stress strain curves are compared, Hooke's law will, even for small deformation, lead to different Young's moduli. Consequently, if the initial stiffness needs to be modelled correctly, viscoelasticity has to be taken into account.

Another example to improve simulation results by considering viscoelasticity is related to the recovery of the viscoelastic material. In pedestrian safety, the lower and upper legform impactors are both made of a metal tubes covered by the viscoelastic Confor[®] foam CF-45. The impactors are fired into a stationary car and the impactor acceleration as well as the knee bending and shearing are measured. Without any doubt, the test result strongly depends on the impactors itself and consequently on the viscoelastic foam behavior. In this test configuration, the viscoelastic stiffness and strengthening for the loading path under compression as well as the slow recovery

and very low rebound resilience of Confor[®] foam CF-45 have a significant influence on the simulation result.

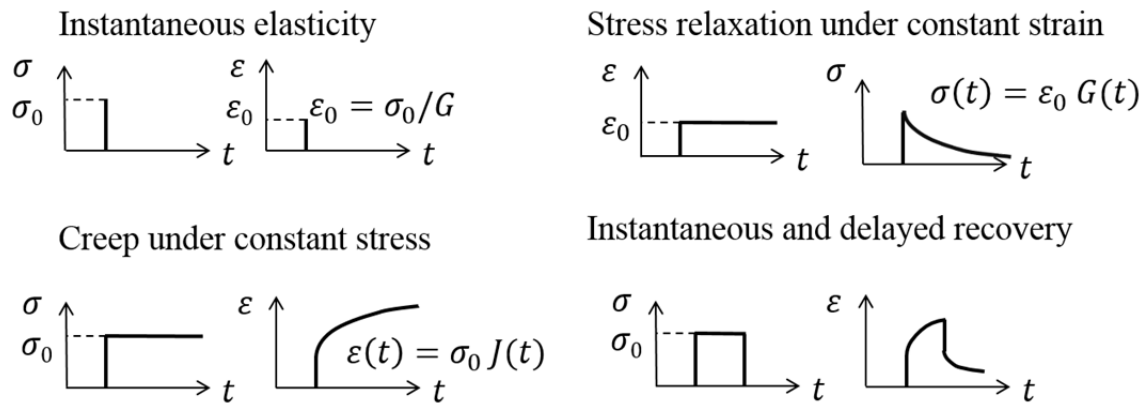


Figure 1: Characteristic behavior of a viscoelastic solid

State of the art in LS-DYNA

Even though viscoelasticity is a common characteristic of polymer materials, this behavior is mainly neglected or incorporated into other material classes for state of the art crashworthiness simulations.

For example, unreinforced thermoplastics are commonly modeled by elastic-viscoplastic material laws as implemented in `*MAT_PIECEWISE_LINEAR_PLASTICITY` (`*MAT_024`) with a von-Mises yield surface or as implemented in `*MAT_SAMP-1` (`*MAT_187`) with a pressure dependent yield surface and non-associated plasticity. To cope with the strain rate dependent initial stiffness of dynamic test data, the yield stress can be shifted to lower values in order to integrate the viscoelastic properties into the viscoplastic material model [1]. As a result, this method will overestimate the plastic strains and cannot be used for general applications.

Rubbers and foams can be modeled with hyperelastic material formulations as provided in `*MAT_SIMPLIFIED_RUBBER` (`*MAT_181`) or in `*MAT_FU_CHANG_FOAM` (`*MAT_083`). These material models also offer a strain rate dependency by an optional table input. For distinct strain rates, corresponding stress-strain curves, respectively force displacement curves, can be referenced [2]. By linear interpolation between the given curves, the table thus spans a stress surface over strain and strain rate. By evaluating this stress surface, very good agreement can be achieved over a wide range of strain rates for the loading path. For the unloading response, a dynamic damage formulation was introduced that makes the material law path-dependent. However, creep, stress relaxation and hysteresis in a viscoelastic sense cannot be represented by this model. [3]

In Figure 2, the force response of a rectangular block specimen to a time-dependent displacement boundary condition is shown. The bottom of the specimen is fixed and the upper side follows the initially harmonic and then constant displacement function. Three different material cards of the model `*MAT_FU_CHANG_FOAM` are used. They all use the same table but differ by the definition of the damage function.

The first one does not use any damage definition and consequently, the unloading path is similar to the loading path except for the small hysteresis due to damping. At load reversal the strain rate crosses zero and in the table evaluation, the stress drops down on the lowest curve. This leads to

oscillations in the force answer. For a constant displacement, the force remains at the same level except for the oscillations. The influence of simple or running strain rate averaging described in [3] cannot be seen at the global output interval and is superposed by the oscillations.

In the second material card, a damage function is defined by the parameters HU and SHAPE. Damage is activated as soon as the current energy at the integration point undercuts the maximum energy at this integration point. Due to the increasing energy, the material response on the loading path is still identical to the first material card, but differs for the unloading path and the following loading. Starting at the first unloading, the stress is lowered by the factor $(1 - d)$ and leads to a softer material response except for the states where the maximum energy is reached again. As a consequence, we can see a hysteresis for the first loading and unloading cycle. However, this is not true for the second cycle where loading and unloading follow the first unloading path. For a constant displacement, the force oscillates around a constant but lower level as for the first material card.

In the third material card, the same damage function as in the second material card is used and the decay option is activated by defining BETAT. The damage decays with the factor $e^{-BETAT \cdot TIME}$ [2]. If the damage relaxes in a time interval corresponding to the time of unloading, the material response for loading and unloading differs for all cycles and shows a hysteretic behavior. In the third material card, the damage relaxation lasts longer than the time of unloading, so the loading path of the second cycle changes from damaged to undamaged path. As a consequence, BETAT cannot be considered as a material constant but as a parameter to adjust the material response to defined boundary conditions.

This example shows that a strain-rate dependent formulation with damage as implemented in *MAT_FU_CHANG_FOAM is not capable to capture the viscoelastic characteristics such as stress relaxation and hysteresis behavior accompanied by energy dissipation.

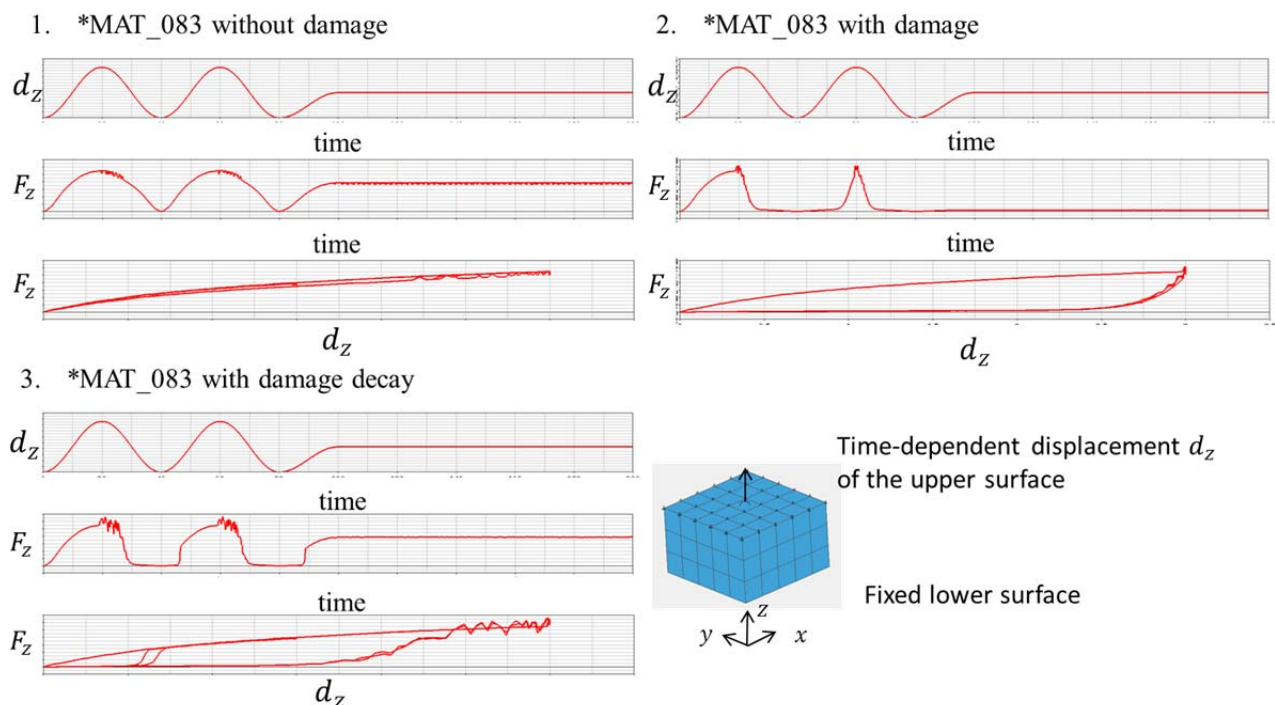


Figure 2: Force response of *MAT_FU_CHANG_FOAM to harmonic and constant displacement with different damage definitions

Linear Viscoelasticity

There are three groups of material laws available in LS-DYNA to model viscoelastic solids. The first one does not use the theory of viscoelasticity but incorporates the viscoelastic effects to some extent in other material classes. This refers to the state of the art in crashworthiness simulation.

The second group of material models for viscoelastic solids consists of linear rheological models (e. g. MAT_006, MAT_061, MAT_076) and belongs to the theory of finite linear viscoelasticity. The third one uses the idea to split the material response into an equilibrium and a memory part. A wide range of material models are constructed that way (e. g. MAT_057, MAT_077, MAT_158). They combine different material classes with a linear viscoelastic overstress of a generalized Maxwell element.

Although the second and third group of material laws are able to model the characteristic properties of viscoelastic solids, their use is restricted. Since the limits of finite linear viscoelasticity can be understood from the theory of linear viscoelasticity for small deformations we will present them under this assumption. For a simple and homogeneous material without aging, the stress σ at the current time t is a functional \mathcal{F} of the strain history $\epsilon(t - u)$

$$\sigma(t) = \mathcal{F}_{u=0}^{\infty}(\epsilon(t - u)). \quad (1)$$

The past time u can be reduced to vary from 0 to t , if the material was in an undeformed state for $t \leq 0$

$$\sigma(t) = \mathcal{F}_{u=0}^t(\epsilon(t - u)). \quad (2)$$

If the stress response to a strain excitation is to be linear, the functional \mathcal{F} must fulfill two conditions. The first one is called stress-strain linearity

$$\mathcal{F}_{u=0}^t(\alpha \epsilon(t - u)) = \alpha \mathcal{F}_{u=0}^t(\epsilon(t - u)) = \alpha \sigma(t) \quad (3)$$

and states that scaling the strain excitation by an arbitrary factor α will increase the stress answer by the same factor. The second condition refers to linearity in time

$$\sigma(t) = \mathcal{F}(\sum_{n=1}^{\infty} \epsilon_n(t - u_n)) = \sum_{n=1}^{\infty} \mathcal{F}(\epsilon_n(t - u_n)) = \sum_{n=1}^{\infty} \sigma_n(t - u_n) \quad (4)$$

and states that the shift of a strain stimuli ϵ_n acting at the time $t - u_n$ also results in a shift of the stress answer σ_n registered at the time $t - u_n$. Furthermore, this condition also states, that the stress answer must be the same if all strain stimuli act as a sum or independently. [4]

Separating the strain rate history into single stimuli and passing to an infinitesimal decomposition leads to the integral form of linear viscoelasticity and is also known as the Boltzmann superposition principle. In the one-dimensional case, the integral form reads

$$\sigma(t) = \int_0^t G(t - u) \dot{\epsilon}(u) du \quad (5)$$

where $G(t)$ is called the stress relaxation function. For the convolution integral in equation 5 we have passed from strain history to strain rate history $\dot{\epsilon}(u) = \frac{\partial \epsilon(u)}{\partial u}$. The equivalent formulation with the convolution of strain history can be recovered via integration by parts

$$\begin{aligned} \sigma(t) &= G(0)\varepsilon(t) - \int_0^t \frac{dG(t-u)}{du} \varepsilon(u) du \\ &= \int_0^t \left(G(0)\delta(t-u) - \frac{dG(t-u)}{du} \right) \varepsilon(u) du. \end{aligned} \tag{6}$$

Both formulations 5 and 6 fulfill the stress-strain linearity (cf. equation 3) and the linearity in time (cf. equation 4).

The actual form of the stress response to a strain rate history depends on the characteristic material function $G(t)$. From a physical point of view the stress response depends more on the recent strain rate history than on the distant past. This is known as the assumption of fading memory and prescribes $G(t)$ to be a monotonically decreasing function.

Explicit stress relaxation functions can be obtained with the help of linear rheological models (cf. Figure 3). For a generalized Maxwell element with a linear spring of stiffness G_{eq} in parallel to N Maxwell units the stress relaxation functions reads

$$G(t) = G_{eq} + \sum_{i=1}^N G_i e^{-\beta_i t}. \tag{7}$$

A Maxwell unit consists of a linear spring with stiffness G_i in series with a linear dashpot of viscosity η_i . The relaxation time for the Maxwell unit results in $\tau_i = G_i/\eta_i$ and characterizes the time when the stress to a step strain excitation has fallen to $1/e \sim 0.369$ of its initial value. Its inverse is called decay constant $\beta_i = 1/\tau_i$. The material models in LS-DYNA using a generalized Maxwell element for the viscoelastic overstress require the stiffness G_i and decay constants β_i as input [2]. The equilibrium stress response is thereby replaced by the underlying material model. This corresponds to replacing the spring with stiffness G_{eq} in the generalized Maxwell element by a different constitutive relation.

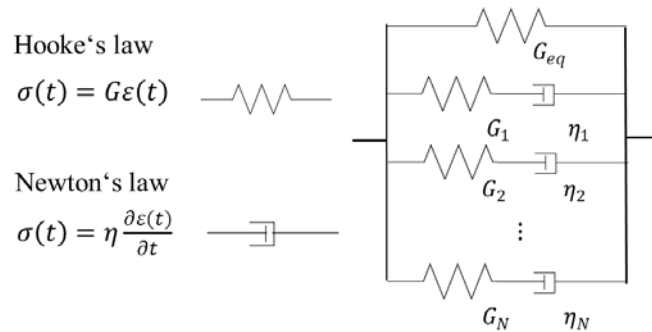


Figure 3: Linear rheological models and a generalized Maxwell element with N Maxwell units

We can use the generalized Maxwell element to analyze the shortcomings of linear viscoelasticity. The stress answer of a generalized Maxwell element to a constant strain rate excitation

$$\varepsilon_1(t) = \dot{\varepsilon}_1 t \tag{8}$$

is given by

$$\sigma_1(t) = \dot{\varepsilon}_1 G_{eq} t + \dot{\varepsilon}_1 \sum_{i=1}^N \frac{G_i}{\beta_i} (1 - e^{-\beta_i t}). \tag{9}$$

In the limit of long test times the answer will approach the asymptote

$$\lim_{t \rightarrow \infty} \sigma_1(t) = \dot{\epsilon}_1 G_{eq} t + \dot{\epsilon}_1 \sum_{i=1}^N \frac{G_i}{\beta_i}. \tag{10}$$

This is the equilibrium answer $\sigma_{eq}(t) = \dot{\epsilon}_1 G_{eq} t$ shifted by the sum $\dot{\epsilon}_1 \sum_{i=1}^N \frac{G_i}{\beta_i}$. Scaling the strain rate by a factor of α

$$\epsilon_2(t) = \alpha \dot{\epsilon}_1 t \tag{11}$$

results in scaling the stress response by the same factor

$$\sigma_2(t) = \alpha \dot{\epsilon}_1 G_{eq} t + \alpha \dot{\epsilon}_1 \sum_{i=1}^N \frac{G_i}{\beta_i} (1 - e^{-\beta_i t}) = \alpha \sigma_1(t) \tag{12}$$

in the stress time diagram (cf. Figure 4). However, this is not valid for the stress strain representation

$$\sigma_1(\epsilon) = G_{eq} \epsilon + \dot{\epsilon}_1 \sum_{i=1}^N \frac{G_i}{\beta_i} (1 - e^{-\beta_i \frac{\epsilon}{\dot{\epsilon}_1}}). \tag{13}$$

There, we cannot judge by simple scaling if the material obeys the stress-strain linearity. Note that the stress strain linearity in the sense of linear viscoelasticity does not refer to a linear relation between stress and strain (cf. Figure 4).

For real materials, the stress strain linearity is limited to certain ranges of the variables stress, strain, time and temperature [6]. In crashworthiness simulation large deformation and a wide range of strain rates arise and consequently, this assumption certainly fails for most materials. This is one of the reasons why the linear viscoelastic material models are little used.

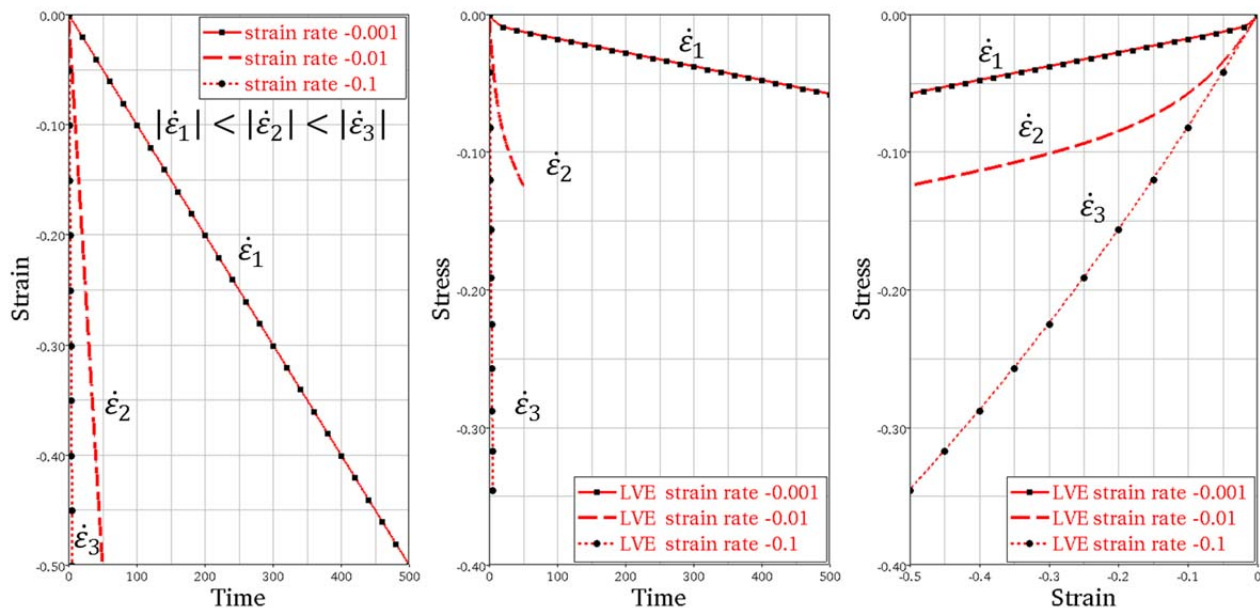


Figure 4: Stress response of a generalized Maxwell element to a constant strain rate excitation in compression

Another reason is the parameter identification. For each Maxwell unit, the stiffness and decay constant must be determined. In LS-DYNA, an internal fit can provide these constants from a stress relaxation curve (e.g. *MAT_076). However, the availability of relaxation tests in industrial environment is restricted.

Nonlinear viscoelasticity based on multiple integral theory

The effects that limit the use of linear viscoelasticity as discussed in the previous section may be of both material and geometric origins. Consequently, we need to pass to a nonlinear constitutive functional and to finite deformation.

The Green-Rivlin model [9] is based on the assumption of a continuous functional that can be approximated by a polynomial of infinite order. Using the Fourier representation of polynomials by integrals, this approximation leads to a multiple integral equation

$$\begin{aligned}
 \mathbf{S}(t) = & \int_0^t \mathbf{K}_1(t - u_1) : \mathbf{E}(u_1) du_1 \\
 & + \iint_{00}^{tt} [\mathbf{K}_2(t - u_1, t - u_2) : \mathbf{E}(u_1)] : \mathbf{E}(u_2) du_1 du_2 \\
 & + \dots \\
 & + \int_0^t \int_0^t \dots \int_0^t \left[[\mathbf{K}_n(t - u_1, t - u_2, \dots, t - u_n) : \mathbf{E}(u_1)] : \mathbf{E}(u_2) : \dots \right] : \mathbf{E}(u_n) du_1 du_2 \dots du_n,
 \end{aligned} \tag{14}$$

where \mathbf{S} is the second Piola-Kirchhoff stress tensor and \mathbf{E} the Green-Lagrangian strain tensor. The convolution kernels \mathbf{K}_n are tensors of order $2(1 + n)$. For the reason of simplicity, the following notation is limited to the second order.

For an isotropic and initially undeformed material, equation 14 reduces to

$$\begin{aligned}
 \mathbf{S}(t) = & \int_0^t A_1(t - u_1) \text{tr}\{\mathbf{E}(u_1)\} \mathbf{I} du_1 + \int_0^t A_2(t - u_1) \mathbf{E}(u_1) du_1 \\
 & + \iint_{00}^{tt} A_3(t - u_1, t - u_2) \text{tr}\{\mathbf{E}(u_1)\} \text{tr}\{\mathbf{E}(u_2)\} \mathbf{I} du_1 du_2 \\
 & + \iint_{00}^{tt} A_4(t - u_1, t - u_2) \text{tr}\{\mathbf{E}(u_1) \cdot \mathbf{E}(u_2)\} \mathbf{I} du_1 du_2 \\
 & + \iint_{00}^{tt} A_5(t - u_1, t - u_2) \mathbf{E}(u_1) \text{tr}\{\mathbf{E}(u_2)\} du_1 du_2 \\
 & + \iint_{00}^{tt} A_6(t - u_1, t - u_2) [\mathbf{E}(u_1) \cdot \mathbf{E}(u_2) + \mathbf{E}(u_2) \cdot \mathbf{E}(u_1)] du_1 du_2 \\
 & + \dots
 \end{aligned} \tag{15}$$

with scalar material functions A_i .

For materials with a zero Poisson's ratio, the constitutive equation can be further simplified to

$$\begin{aligned} \mathbf{S}(t) &= \int_0^t A_2(t - u_1) \mathbf{E}(u_1) du_1 \\ &+ \iint_{00}^{tt} A_6(t - u_1, t - u_2) [\mathbf{E}(u_1) \cdot \mathbf{E}(u_2) + \mathbf{E}(u_2) \cdot \mathbf{E}(u_1)] du_1 du_2 \\ &+ \dots, \end{aligned} \quad (16)$$

where all terms involving the trace of the Green Lagrangian strain tensor are omitted. If the material functions are symmetric in their arguments [5] and additionally are of the product form

$$\begin{aligned} A_2(t - u_1) &= \tilde{M}_1(t - u_1) \\ A_6(t - u_1, t - u_2) &= \tilde{M}_2(t - u_1) \tilde{M}_2(t - u_2) \\ &\vdots \end{aligned} \quad (17)$$

the Green-Rivlin model finally reduces to

$$\begin{aligned} \mathbf{S}(t) &= \int_0^t \tilde{M}_1(t - u_1) \mathbf{E}(u_1) du_1 + \left[\int_0^t \tilde{M}_2(t - u_1) \mathbf{E}(u_1) du_1 \right]^2 \\ &+ \left[\int_0^t \tilde{M}_3(t - u_1) \mathbf{E}(u_1) du_1 \right]^3 + \left[\int_0^t \tilde{M}_4(t - u_1) \mathbf{E}(u_1) du_1 \right]^4 \\ &+ \left[\int_0^t \tilde{M}_5(t - u_1) \mathbf{E}(u_1) du_1 \right]^5. \end{aligned} \quad (18)$$

Due to the properties of matrix polynomials [7] no more than terms of the fifth order need to be retained for isotropic materials. Consequently, equation 18 represents the complete constitutive equation for the Green-Rivlin model with respect to the aforementioned assumptions. This formulation still relies on linear convolution integrals. Their exponent j represents an j – fold contraction of the tensors with itself and builds up the nonlinearity.

Finite linear viscoelasticity is also included in this model, if only the first order term with material function \tilde{M}_1 is retained.

In order to compare the formulation of fifth order with the generalized Maxwell element of linear viscoelasticity we use the same material function for the first order term (cf. equation 7)

$$G_1(t) = G_{eq} + \sum_{i=1}^N G_{1i} e^{-\beta_{1i} t} \quad (19)$$

and omit the equilibrium modulus for higher order terms

$$G_j(t) = \sum_{i=1}^N G_{ji} e^{-\beta_{ji} t}. \quad (20)$$

The transition from strain to strain rate formulation is analogous to linear viscoelasticity

$$\tilde{M}_j(t) = \left(G_j(0) \delta(t - u) - \frac{dG_j(t-u)}{du} \right). \quad (21)$$

For uniaxial loading with a constant strain rate $E_{11}(t) = \dot{E}_1 t$ the stress response is given by

$$s_{11}^{cst\ slope}(t) = \dot{E}_1 G_{eq} t + \sum_{j=1}^5 \left(\dot{E}_1 \sum_{i=1}^N \frac{G_{ji}}{\beta_{ji}} (1 - e^{-\beta_{ji} t}) \right)^j. \quad (22)$$

The stress answer differs for negative or positive strain rate, respectively for compression and tension.

Furthermore, this formulation is capable to represent saturation. Saturation in this context signifies that an increase in the excitation will lead to a smaller and smaller increase in the material response. For example, if we look at the stress response

$$s_{11}^{relax}(t) = E_1 G_{eq} + \sum_{j=1}^5 \left(E_1 \sum_{i=1}^N G_{ji} e^{-\beta_{ji} t} \right)^j \quad (23)$$

to a constant step of strain $E_{11}(t) = E_1 \mathcal{H}(t)$, the stress difference between two excitations E_1 and $E_2 = \alpha E_1$ differing by a constant positive factor α will decrease with an increasing amount of the excitation E_1 . In Figure 5, this saturation is compared to linear viscoelasticity where the factor α is also present in the difference of the stress response. The amount of the compressive stress for the linear viscoelastic model exceeds the stress response for the nonlinear viscoelastic Green Rivlin model.

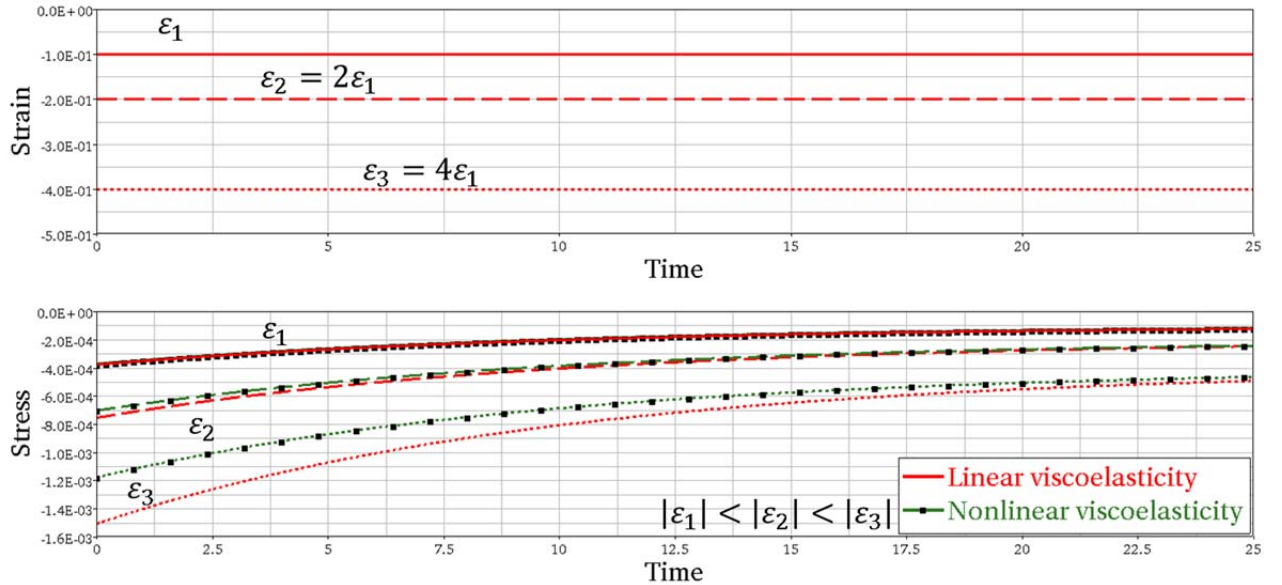


Figure 5: Comparison of the stress response $s_{11}^{relax}(t)$ of linear viscoelasticity and of nonlinear viscoelasticity with the same response for the strain step $E_{11}(t) = \varepsilon_1 \mathcal{H}(t)$

In a mathematical way, saturation occurs if the first derivative of the stress response with respect to the excitation is positive

$$\frac{\partial s_{11}^{relax}}{\partial E_1} > 0 \quad (24)$$

and the second derivative is positive for negative excitation and negative for positive excitation

$$\frac{\partial^2 s_{11}^{relax}}{\partial E_1^2} \geq 0 \text{ for } E_1 < 0 \text{ and } \frac{\partial^2 s_{11}^{relax}}{\partial E_1^2} \leq 0 \text{ for } E_1 > 0. \tag{25}$$

For $j = 1$, the conditions for the second derivative cannot be fulfilled and therefore, linear viscoelasticity is not capable to represent saturation behavior.

Modeling of Confor[®] Foam

Polymer materials may exhibit viscous and elastic properties in any ratio. The time the molecular units of the polymer chains need to change their place does not only depend on their molecular structure but also on the operating conditions such as temperature, humidity and strain rate.

In urethane foam Confor[®] CF-45, material and structural properties lead to pronounced damping and shock-absorption capabilities. On the one hand, the viscous chain movements close to glass transition temperature maximize the dissipated energy. On the other hand, the open-celled foam structure leads to favorable pressure distribution and a high energy absorption under compression at a constant stress level.

To identify the material properties for crashworthiness simulation, quasistatic and dynamic tests under uniaxial tension and compression loading at rectangular block specimens of Confor[®] CF-45 are performed at the Fraunhofer Institute for High-Speed Dynamics, Ernst-Mach-Institut, EMI, at Freiburg. While the dynamic tests cover the range of strain rates of an impact simulation and reveal the viscous effects, the characterization under tension and compression traces back to the foam structure.

Under compression, three regimes of the quasistatic test curve of Confor[®] foam can be distinguished (cf. Figure 6). At first, the elastic bending of cell walls dominates the behavior. Then, cell walls start buckling and further deformation occurs at nearly constant stress level as buckling percolates through the material. This second part is called plateau regime. The last regime is characterized by the total collapse of the cell structure that leads to full densification and is accompanied by a strong stress increase. Due to its cell structure, Confor[®] foam shows very little lateral expansion under compression and its Poisson’s ratio can be assumed to be close to zero. Under tension, the quasistatic response for Confor[®] foam can be represented by a linear stress-strain curve with a constant modulus.

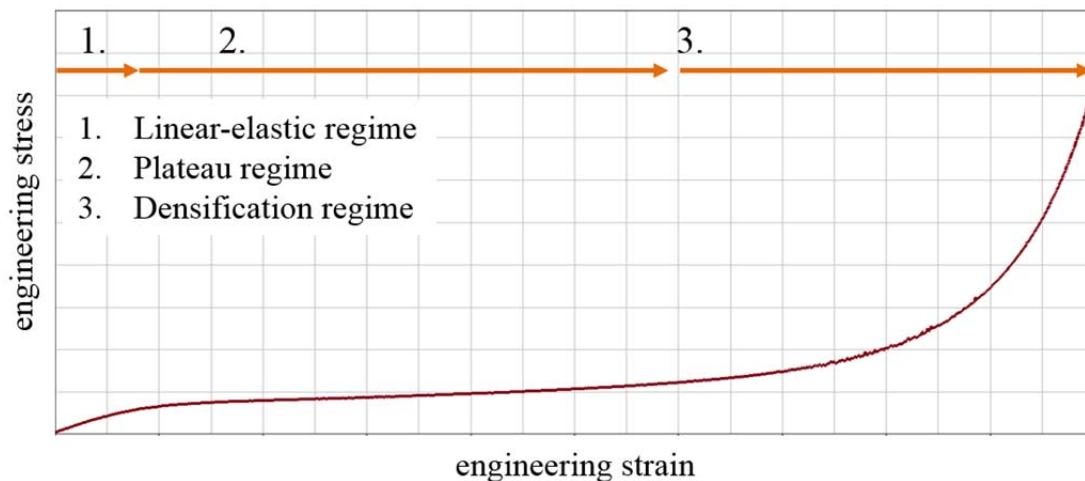


Figure 6: Engineering stress-strain curve for Confor[®] CF-45 from quasistatic compression test

For the user-defined material model, this behavior is included in the hyperelastic equilibrium formulation based on the work of Chang [8] and formerly implemented as *MAT_FU_CHANG_FOAM in LS-DYNA (*MAT_083).

The non-equilibrium stress of the user-defined material model is given by the nonlinear viscoelastic formulation for foams developed in the previous section (cf. equation 18). The parameter identification for the viscous behavior is done with respect to the second Piola Kirchhoff stress and Green Lagrangian strain. Therefore, all force-displacement curves are transformed in these stress and strain measures and the quasistatic answer is subsequently subtracted from the dynamic tests.

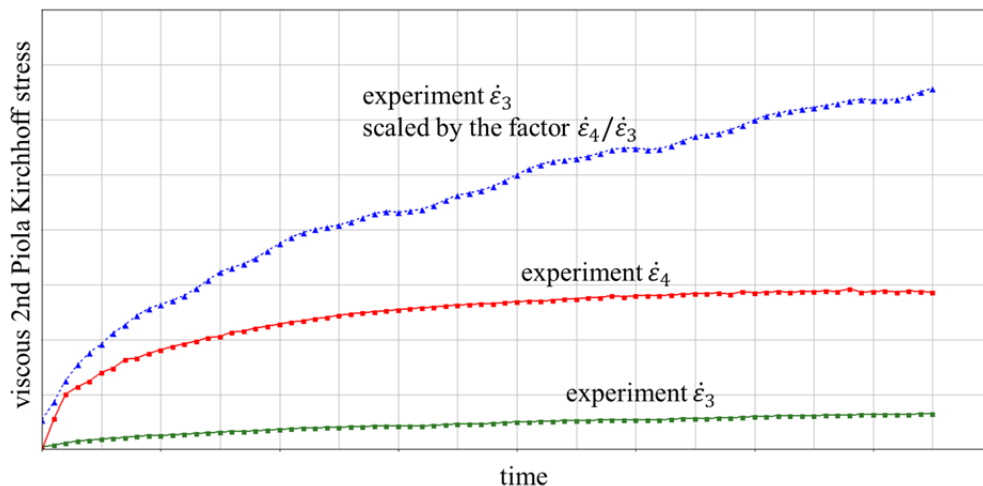


Figure 7: Confor[®] CF-45 stress answer at strain rate $\dot{\epsilon}_3$ and $\dot{\epsilon}_4$. If the material was linear viscoelastic, the experimental curve $\dot{\epsilon}_4$ would coincide with the curve $\dot{\epsilon}_3$ scaled by $\dot{\epsilon}_4/\dot{\epsilon}_3$.

The nonlinearity of the Confor[®] test data is shown in Figure 7. The viscous second Piola Kirchhoff stress is plotted over the time for two distinct strain rates $\dot{\epsilon}_3$ and $\dot{\epsilon}_4$. Respecting proprietary data, the axes do not show any specific values.

In the stress time representation, the linearity of the experimental data can be evaluated. If the material was linear viscoelastic, the experimental curve at strain rate $\dot{\epsilon}_4$ would coincide with the experimental curve at strain rate $\dot{\epsilon}_3$ scaled by the factor $\dot{\epsilon}_4/\dot{\epsilon}_3$. However, the material testing at strain rate $\dot{\epsilon}_4$ leads to a lower stress response and represents an example of saturation. As a consequence, the assumption of linear viscoelasticity clearly fails for Confor[®] foam.

The viscous stress-strain curves (cf. Figure 8) are the basis for the parameter identification. The Green-Rivlin model of fifth order with material functions according to equations 19 and 20 may depend on numerous variables. Therefore, the optimization software LS-OPT[®] is used and the first results of the parameter identification are shown in Figure 8. In order to test the general properties of the material model and to reduce the computational costs, the optimization is set up with the objective to minimize the error between the model answer and the test results for strains up to 20%.

For the compression tests, the viscous stress in simulation is overestimated in comparison to the experimental values for the second strain rate and is in acceptable agreement for the third strain rate. For the tensile tests, the simulation with the Green Rivlin model for foams is in very good agreement with the experimental test curves for all strain rates and the material model is able to reproduce the initial stiffness correctly.

However, if the simulation is extended to higher strain or strain rates, experimental and simulation results may diverge not only because of invalid parameters but also because of localization phenomena. This is related to the fact that the stability conditions

$$\frac{\partial \sigma}{\partial E} > 0 \quad \text{and} \quad \frac{\partial \sigma}{\partial \dot{E}} > 0 \quad (26)$$

are not automatically fulfilled for all relevant strain and strain rates. Therefore, the parameter identification must be conducted with these constraints.

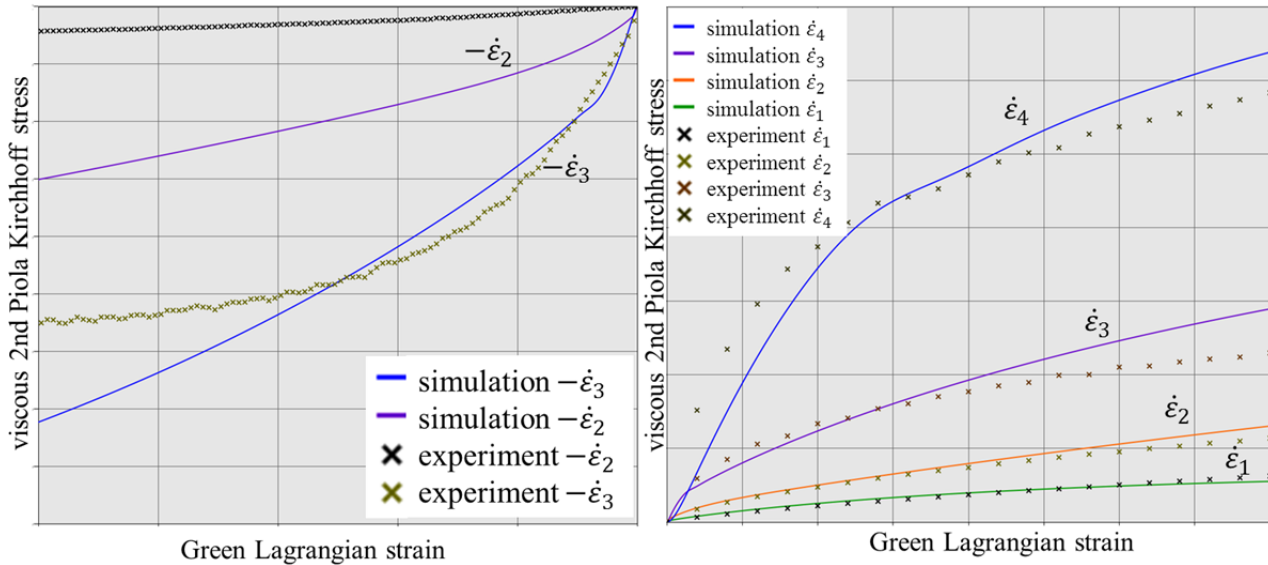


Figure 8: Comparison of simulation and experimental viscous stress-strain curves of Confor[®] CF-45 from compression test (left) and tension test (right) at different strain rates

With regard to the characteristics of a viscoelastic solid, the same example of a rectangular block specimen subjected to a harmonic and constant displacement boundary condition as for *MAT_FU_CHANG_FOAM (cf. Figure 2) is simulated. The results for the user-defined material model with the parameters of Figure 8 are shown in Figure 9.

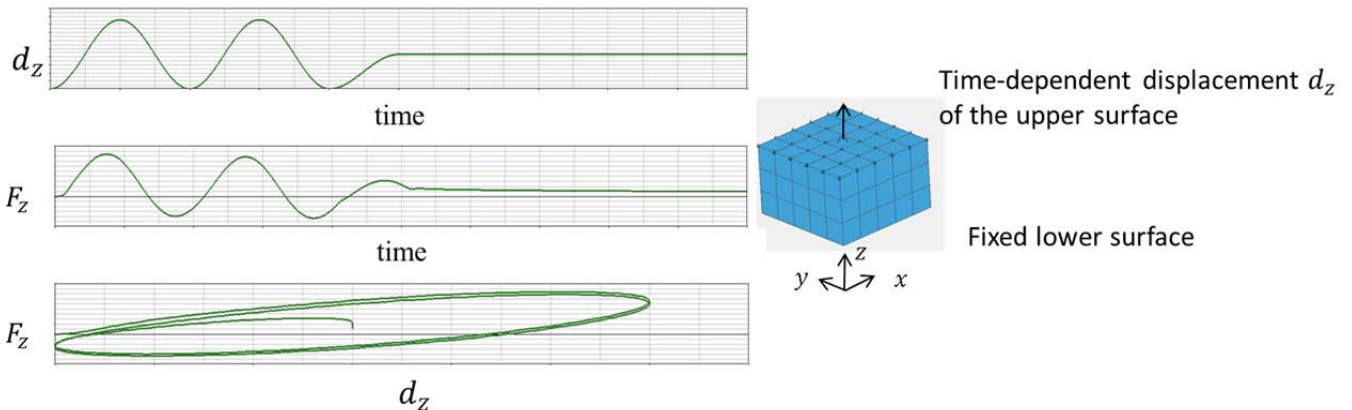


Figure 9: Force response of the user-defined nonlinear viscoelastic foam model to harmonic and constant displacement

For the harmonic displacement excitation, the force response is also periodic but differs by a phase shift. That is why the maximal force and the maximal displacement do not coincide in the force displacement diagram. The maximal force is reached before the maximal displacement is applied because of the decreasing displacement rate.

In addition, the unloading path differs from the loading path for both cycles and the unloading leads to compressive stress although the specimen is still subjected to tensile strain exclusively. This is a major difference to *MAT_FU_CHANG_FOAM where tensile strain always leads to tensile stress. The second cycle resembles the first cycle but is not identical as the stationary state is not yet reached where transient terms can be neglected.

Finally, for a constant displacement the stress relaxes to its equilibrium value.

Conclusions

A new user-defined material model for foam modeling has been implemented in LS-DYNA. It consists of an equilibrium hyperelastic stress response and of a non-equilibrium stress response based on the multiple integral theory by Green and Rivlin. This constitutive model is capable to represent nonlinear viscoelastic material behavior such as stress relaxation, creep and recovery as well as saturation.

The model is used to simulate the behavior of the urethane foam Confor[®] CF-45 and reproduces the stress-strain curve in the range up to 20% Green Lagrangian strain in good agreement. However, due to the polynomial structure, the constitutive equation does not ensure material stability for any material functions and for all strain and strain rates. Thus, the use of the parameter set is limited to the validated range of strain and strain rates.

Consequently, for further parameter identification, the choice of parameters must be limited to fulfill the stability conditions for the complete range of strain and strain rates of the desired application. These constraints as well as the number of unknowns resulting from the parameterization of up to five material functions require the use of an optimization procedure.

In addition, it is not obvious that the parameterization of the material functions will lead to good agreement between simulation and experimental stress strain curves over the whole range of strain and strain rates. Therefore, future investigations are planned to use different sets of parameters for certain time intervals.

Acknowledgment

We would like to thank Trelleborg Applied Technology, United Kingdom, for providing the sample material Confor[®] CF-45.

References

- [1] Schöpfer, J. (2001). 'Spritzgussbauteile aus kurzfaserverstärkten Kunststoffen: Methoden der Charakterisierung und Modellierung zur nichtlinearen Simulation von statischen und crashrelevanten Lastfällen', PhD Thesis, University of Kaiserslautern
- [2] LS-DYNA User Manual and Theoretical Manual, Livermore Software Technology Corporation
- [3] Kolling, S., P. A. Du Bois, D. J. Benson & W. W. Feng (2007). 'A tabulated formulation of hyperelasticity with rate effects and damage.' Computational Mechanics 40(5), pp. 885-899.
- [4] Tschoegl, N. W. (1989). The Phenomenological Theory of Linear Viscoelastic Behavior. Springer.

[5] Lockett, F. J. (1965). 'Creep and stress-relaxation experiments for non-linear materials.' International Journal of Engineering Science 3 (1), pp. 59-75

[6] Findley, W. N., J. S. Lai & K. Onaran (1976). 'Creep and relaxation of nonlinear viscoelastic materials.' volume 18 of Applied mathematics and mechanics. North Holland Publishing Company.

[7] Spencer, A. & R. Rivlin (1959). 'Further results in the theory of matrix polynomials.' Archive for Rational Mechanics and Analysis 4(1), pp. 214-230

[8] Chang, F. S. (1995). 'Constitutive equation development of foam materials.' PhD Thesis, Wayne State University, Michigan, US

[9] Green, A. E. & R. S. Rivlin (1957). 'The mechanics of non-linear materials with memory -Part I.' Archive for Rational Mechanics and Analysis 1(1), pp. 1- 21.